CrossMark

Combination of NMR and MRI Techniques for Non-invasive Assessment of Sea Cucumber (*Stichopus japonicas*) Tenderization During Low-Temperature Heating Process

Xiuping Dong[1,2,3,4] • Yan Li[1,2,3,4] • Yong Li[1,3,4] • Liang Song[1,3,4] • Shasha Cheng[1,2,3] •
Dongmei Li[1,2,3,4] • Bei-Wei Zhu[1,2,3,4] • Dayong Zhou[1,2,3,4] • Mingqian Tan[1,2,3]

Abstract The purpose of this study was to develop and test the combination of nuclear magnetic resonance (NMR) and magnetic resonance imaging (MRI) method to assess the proton changes of sea cucumber body wall during low-temperature heating process. NMR relaxometry and MRI measurements indicated a significant proton change in the internal structure for sea cucumber body wall when the heating temperature increased from 45 to 55 °C. Differential scanning calorimetry (DSC) analysis revealed that the denaturation temperature of sea cucumber body wall was in the range of 45–55 °C with an endothermic peak at 51 °C, which is in accordance with the result observed in NMR and MRI. Rheological study showed similar trend to the DSC thermogram. The band change in amide I region of Fourier transform infrared (FTIR) spectra indicated the decrease in α-helix content and possible formation of other secondary structures. Scanning electron microscopy (SEM) further confirmed that the low-temperature heating did induce microstructure changes. The analysis of the Ringer s soluble fraction (RSF), enzyme-labile fraction (ELF), and total unaltered fraction (TUF) for sea cucumber body wall during low-temperature heating provided more detailed information on the cause of structure change observed in NMR and MRI. The NMR parameters were highly correlated with the rheology storage modulus (G′), relative enzymatic assay parameters, RSF, ELF, and TUF. All these results demonstrated that it could be possible to use NMR and MRI to assess sea cucumber tenderization during low-temperature heating process.

Keywords Sea cucumber · Low-field NMR · MRI · Low-temperature heating · Collagen fiber · Tenderization

Introduction

Sea cucumber (*Stichopus japonicas*) is a worm-like echinoderm with soft body and belongs to the class Holothuroidea found in benthic areas across the world's oceans. It has been become an important human food and pharmaceuticals in parts of Asian countries (Kim and Himaya 2012). Sea cucumber is also perceived as a tonic food for thousands of years (Zhou et al. 2006). The total output of sea cucumber has reached more than 200,000 tons in China in 2014 (Yearbook 2009). Besides the traditional dried sea cucumber, new products like instant sea cucumber start to emerge as consumer favorite, which is more convenient for consumption. The instant sea cucumber retains more nutrients than dried sea cucumber because it avoids a long-time rehydration process and has unique texture. However, the instant product varies considerably in quality, and some of them are hard to masticate because of the inappropriate cooking treatment.

Tenderization is a common technology in meat processing to break down collagens in cooking for better palatability. Tenderness is regarded as one of the most important attributes that affect the eating quality of meat. Previous reports have shown positive correlation between taste and overall customer satisfaction (Naganathan et al. 2008). Customers would be

✉ Mingqian Tan
2468750030@qq.com

1   School of Food Science and Technology, Dalian Polytechnic University, National Engineering Research Center of Seafood, 1 Qinggongyuan, Ganjingzi District, Dalian 116034, China

2   Engineering Research Center of Seafood of Ministry of Education of China, Dalian 116034, China

3   Liaoning Key Laboratory of Seafood Science and Technology, Dalian 116034, China

4   National Research and Development Branch Center for Shellfish Processing (Dalian), Dalian 116034, China

ready to pay more for a tender meat product. Numerous investigations have examined meat, e.g., beef (Lomiwes et al. 2014), pork (Van Laack et al. 2001), chicken (Yogesh and Ali 2014), tenderization, and there are various factors like temperature, pH value, and enzymes contributed to meat tenderness. On one hand, the nature for meat tenderization is a limited hydrolysis of muscle tissue by endogenous proteases. On the other hand, the physicochemical factors can also significantly affect the tenderization. Unlike beef, pork, or chicken meat, sea cucumber body wall is mainly mutable connective tissue (MCT) which have a large proportion of collagen (Saito et al. 2002). There have been recent reports suggesting that collagen may be unstable due to temperature (Leikina et al. 2002), ultraviolet radiation (Rabotyagova et al. 2008), and enzymes (Zhou et al. 2014). Although the effects of autolysis have been studied extensively, the non-enzymatic tenderization during low-temperature heating for sea cucumber body wall is hardly mentioned in literature. Thermal ripening is key processing step in production of instant sea cucumber. Temperature effect on collagen protein is a very important factor related with physiochemical properties of sea cucumber protein. It has been supposed that changes in textural and functional properties such as apparent viscosity, extractability, or water holding capacity are related to protein denaturation and/or aggregation (Herrero et al. 2005). Despite its importance of tenderization, it is important to illustrate the change of body wall proteins during low-temperature heating for product quality control.

Conventional techniques, such as rheological measurement, differential scanning calorimetry (DSC), Fourier transform infrared spectroscopy (FTIR), and scanning electron microscopy (SEM), have proved success in assessment of meat tenderization (Bertram et al. 2006; Lee et al. 1990; Liu et al. 2012). They still suffer from some disadvantages such as time consuming, sample destructive, and lack of visualization information for monitoring meat tenderization. Therefore, it is highly desired to develop a non-invasive visualization method for assessment of body wall tenderization of sea cucumber during low-temperature heating process. Recently, low field nuclear magnetic resonance (LF-NMR) and magnetic resonance imaging (MRI) techniques have become powerful tools in monitoring food processing due to its non-invasive characteristics, high reproducibility, and sensitivity (Marcone et al. 2013). NMR can reflect the distribution of water pools with different relaxation times in foods (Carneiro et al. 2013) based on the measurement of resonant radio frequency absorption by non-zero nuclear spins (protons have the spin $I = 1/2$) in the presence of an external static magnetic field. It uses spin-lattice relaxation time (T_1) and spin-spin relaxation time (T_2) to reflect the features of proton relaxation (Zhang and McCarthy 2012). Many food samples, such as pork (Li et al. 2012), beef (Santos et al. 2014), and hake muscle (Sánchez-Valencia et al. 2015), have been investigated based on their hydrogen proton difference. NMR will become increasingly

useful as a non-invasive tool for process monitoring and quality control through continued development in low-field permanent magnet technology. On the other hand, MRI, another type of NMR technology, has been extensively clinically used to detect structural abnormalities of the body (Nakano et al. 2012). It has also been increasingly used to explore food analysis and food processing (Shao and Li 2010). As an accurate and non-destructive method for visualizing the internal food structure, MRI has been combined with NMR to gain more information like water uptake, mobility and distribution, and simultaneous internal structural changes in food analysis and processing (Patel et al. 2015). The combined NMR and MRI technique has been successfully used for the analysis of egg white gel (Liu et al. 2013), navy beans (Zhang and McCarthy 2013), etc. This cannot only provide the non-invasive analysis of proton changes, but also the visualization information of the structural changes during food processes.

The main purpose of the current study was to examine the proton changes of sea cucumber body wall during low-temperature heating tenderization process using the combined NMR and MRI. Our previous study has indicated that the tenderness of sea cucumber can be improved after low-temperature heating tenderization treatment followed by a rapid high-temperature ripening step (Zhu et al. 2013). However, to the best of our knowledge, no research endeavors are yet executed for analysis of body wall tenderization of sea cucumber using such fast and visualization method. The results of NMR and MRI were correlated with those from DSC, FTIR, and SEM measurements. Our specific objectives were to (1) establish a fast and non-invasive method for the assessment of the tenderization of sea cucumber body wall; (2) analyze the correlation between NMR relaxometry and texture features extracted from rheological measurement, structure changes observed in DCS, rheology, FTIR, and SEM analysis; and (3) provide more insights into the relationship of physicochemical properties of the collagen structure changes as well as enzyme solubility of the collagen molecule.

Materials and Methods

Materials and Chemicals

Fresh sea cucumbers (*S. japonicas*, 90 ± 5 g, 15 ± 2 cm apiece) were obtained from Changhai county of Dalian, China. They were transported to the local market (Liujiaqiao) in seawater, and then to our laboratory in a plastic bag with ice. The sea cucumbers were kept in ice water for 30 min before removing the viscera. Sea cucumber body wall samples were cut from the approximately geometric center area of each sea cucumber. Each experiment requires at least 7 sea cucumbers. Pronase (Pronase E, Sigma P-5147, Lot 43H0731) was purchased from Sigma–Aldrich (Sigma–Aldrich, Co., Shanghai,

China); other common chemicals used in this work were from commercial sources and are of analytical grade.

NMR and MRI Measurements

Sea cucumber samples with a size of approximately 1 × 1 × 3 cm were heated at 35, 45, 55, 65 °C for 30 min, respectively. After being cooled to room temperature, the samples were blotted with absorbent paper to remove excess water on their surface. NMR and MRI were performed as described by our previous work (Geng et al. 2015). Briefly, transverse relaxation (T_2) measurement was performed on a bench top MiniMR-Rat analyzer (Suzhou Niumag Analytical Instrument Co., Suzhou, China) equipped with a 0.5 T permanent magnet corresponding to a proton resonance frequency of 23.2 MHz at 32 °C. The body wall sample of sea cucumber was placed on NMR bed by using a 30 mm diameter radio frequency coil to collect Carr-Purcell-Meiboom-Gill (CPMG) decay signals, with 90° and 180° pulses of 13 and 26 μs, respectively, τ-value (time between 90° and 180° pulses) of 100 μs. Data from 15,000 echoes were acquired as 3 scan repetitions. The repetition time between subsequent scans was 8 s, and each measurement was performed in triplicate. Distributed multi-exponential fitting of CPMG decay curves was performed in MultiExp Inv analysis software (Suzhou Niumag Analytical Instrument Co., Suzhou, China). The multi-exponential fitting analysis was performed on the relaxation data in the software algorithm, the SRIT analysis, to get a better fitting. From the analysis, the transverse relaxation times for each process were calculated from the peak position, and the area under each peak, corresponding to the proportion of water molecules exhibiting that relaxation time, was determined by cumulative integration.

MRI data was also acquired on 0.5 T (permanent magnet) MiniMR-Rat (Suzhou Niumag Analytical Instrument Co., Suzhou, China) equipped with a 30 mm radio frequency coil 32 °C. T_1 and T_2 weighted images were acquired using SE imaging sequence, with T_1 weighted image echo time (TE) of 19 ms and repetition time (TR) of 300 ms, T_2 weighted image echo time (TE) of 50 ms and repetition time (TR) of 1600 ms, respectively. Field of view (FOV) of 100 mm × 100 mm, slice width: 2.5 mm, slice Gap: 0.5 mm, average: 4, read size: 256, phase size: 192 were used for magnetic resonance imaging.

DSC Analysis

Sea cucumber body wall samples ($N = 7$) were homogenized by oscillating mill (MM400, Retsch Co. Std, Germany). The body wall pastes (400 mg) were weighed into aluminum pans and hermetically sealed. The net heat energy (enthalpy, $\triangle H$), the onset (T_{onset}), and maximum (T_{max}) temperature for endothermic transition of myosin were tested using differential scanning calorimeter (SETARAM Instrumentation, Caluire,

France). The samples were heated from 10 to 70 °C at heating rate of 1 °C/min. An empty sample pan was used as the reference. The T_{max} temperature was estimated from the thermogram using the software of DSC Manager Series. All treatments were tested in triplicate.

Oscillation Dynamic Rheology

Dynamic rheological studies were performed on a discovery dynamic rheometer (TA Instrument, New Castle, DE, USA). A 40-mm parallel steel plate geometry with a 1 mm gap was used, and the body wall mixture was surrounded by distill water to prevent loss of moisture during heating. Samples were heated at a rate of 1 °C/min from 20 to 80 °C. This temperature ramp tests were done at a fixed frequency of 1 Hz with a fixed stress of 0.6 Pa to ensure the integrity of gel network. Storage modulus (G′), loss modulus (G″), and tangent phase angle (tanδ = G″/G′) were recorded. All treatments were tested in triplicate. To determine the influence of the heating time on structural changes, time sweep tests were additionally performed at 45 °C and at various times up to 120 min.

Enzyme Digestion

Body wall samples ($N = 7$) were homogenized by oscillating mill. After being heated at 35, 45, 55, 65 °C for 30 min, respectively, the body wall samples were submitted for enzymatic digestion after cooling down to room temperature. Ringer's soluble fraction (RSF), enzyme-labile fraction (ELF), and total unaltered fraction (TUF) of sea cucumber body wall were determined according to the procedures of the literature (Powell et al. 2000) with a slight modification. Briefly, 5.25 mL of strength Ringer s solution at 4 °C was added to 1 g of body wall sample in a 25 mL centrifuge tube, and the mixtures were vortexed for 2 min. The solutions were kept at 20 °C for 30 min, and then centrifuged at 6000g for 10 min. The residue of Ringer's insoluble fraction was placed in a small screw-top tube, and 5 mL of suspension of pronase was added. The activity of the enzyme was 2.7 units per mg. The mixture was digested overnight at 20 °C with shaking. Supernatant and residue were decanted for hydroxylproline determination by using a UV-Visible Spectrophotometer (UV230, Purkinje General Corporation, Beijing, China) at 560 nm as reported previously (Powell et al. 2000).

FT-IR Analysis

Collagen fibril protein was extracted according to the method by Nagai T (Nagai and Suzuki 2000) for FTIR measurement. The extracted collagen fibril sample (~10 mg) was dissolved in a 1.5 mL of D_2O and heated at 45 °C, through the 15- to 120-min interval. Infrared spectra were recorded on a Perkin-

Elmer Spectrum 100 Fourier transform infrared spectrometer (Perkin Elmer Inc., USA). The sample solutions were injected in a CaF_2 cell with 50 μm Teflon spacer. A 32-scan cumulant was collected by single-beam mode with a 2 cm^{-1} resolution. Amide I band (1700–1600 cm^{-1}) from the C–O stretching vibrations was used to demonstrate the collagen fibril change upon heating at 45 °C.

Scanning Electron Microscopy Characterization

The heated body wall samples were cut into $1 \times 1 \times 1$ cm^3 rectangular prism blocks by using raw body wall sample as a control after being heated at 45 °C for 15, 30, 60, and 120 min, respectively. The fixed samples were dehydrated with ethanol and coated with gold palladium in a vacuum. Measurements were conducted with a JEOL scanning electron microscope (JSM-840; JEOL Co. Ltd., Japan).

Statistical Analysis

Statistical analysis of the significance results was performed using Statistical Analysis System IBM SPSS (Statistical Package for the Social Sciences) statistics v16 software (IBM Corporation, NY). One-factor analysis of variance (ANOVA) was performed for each of the parameters. Correlations between factors were performed. All the diagrams were plotted using Origin 8.5 software.

Results and Discussion

NMR and MRI Analysis

Figure 1a shows the CPMG relaxation curves for sea cucumber body wall, and the trend was closely associated with the different physicochemical properties in the samples. The main

constituent of fresh sea cucumber body wall, water, is mainly held within the highly organized structures of collagen protein. Definite structural changes in proteins during tenderization process (low-temperature heating) are associated with simultaneous alterations in the chemical–physical properties of the water within the sea cucumber body wall. NMR relaxometry is a non-destructive method that enables probing the mobility of protons. The mobility of proton molecules is related to the spin-lattice relaxation time (T_1) and the spin-spin relaxation time (T_2). The transverse relaxation (T_2) would be expected to be an excellent tool to quantify the heating effects on the water mobility and distribution of sea cucumber body wall. The results presented here indicate that LF NMR T_2 relaxometry is actually sensitive to different heating temperature which are known to affect water distribution, alter collagen protein morphology and produce structural changes. In order to obtain a noticeable difference among these sea cucumber body walls, T_2 relaxation spectra were produced by multi-exponential fitting of the transverse relaxation raw data shown in Fig. 1a. As shown in Fig. 1b, three distinct water populations are observed for the samples treated at different temperatures. The three relaxation populations were assigned to three water states, that is, bound water ($T_{21} \sim 0$–10 ms), immobile water (or myofibrillar water, $T_{22} \sim 30$–80 ms), and also expelled "bulk" free water ($T_{23} \sim 180$–360 ms), respectively. The existence of three group water in sea cucumber is in agreement with our previous report (Geng et al. 2015). The transversal relaxation times (T_{21}, T_{22}, T_{23}, ms) and corresponding amplitudes (A_{21}, A_{22}, A_{23}, arbitrary units) from multi-exponential analysis of T_2 relaxation data of sea cucumber body wall are summarized in Table 1. Upon heating, there are significant changes (5.36–1.22 ms) for T_{21} relaxation time. A marked decreasing of T_{22} relaxation times from 71.26 to 31.02 ms is found along with the temperature increase from room temperature to 65 °C. The decrease in T_{22} values at the later stage of heating may reflect the structural changes due to
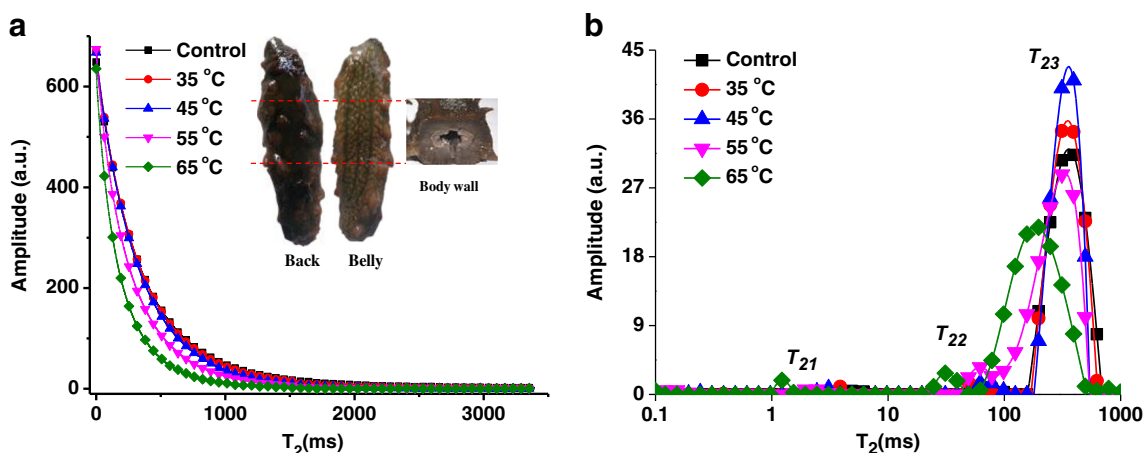

Fig. 1 CPMG decays (**a**) and continuous distribution of the transversal relaxation times (T_2) (**b**) in sea cucumber body walls after heating at different temperature for 30 min. *Inset* shows the photograph of sea cucumber body wall. The temperature was 25 °C for control sample, similarly hereinafter

Table 1 NMR parameters obtained for sea cucumber body wall at different temperature (A_{21}, A_{22}, and A_{23} represented the area percentages of bound water, immobile water, and free water, respectively)

Temperature (°C)	T_{21}	T_{22}	T_{23}	A_{21}%	A_{22}%	A_{23}%
Control	5.36	71.26	359.07	0.73	1.43	97.84
35	3.70	54.01	342.86	0.87	2.41	96.72
45	2.81	68.04	359.04	1.15	2.74	96.10
55	2.23	62.04	327.38	2.90	5.69	91.42
65	1.22	31.02	188.04	4.85	4.30	90.85

shrinkage and toughening of the body wall as well as moisture loss due to heating (Shaarani et al. 2006). T_{23} did not change a lot in low-temperature sample (35 and 45 °C) and decreased sharply when the temperature reached 55 °C. It has been reported that the mobility of the present phases of spins in the system changes usually if protein solutions are heated above its denaturation temperatures (Goetz and Koehler 2005). Among them, T_{22} and T_{23} decrease at 35 °C and then increase at 45 °C, indicating that the state of water in sea cucumber body wall is more active and structure change occurred. Moreover, the corresponding amplitudes A_{21}, A_{22}, and A_{23} changed significantly (Table 1). A_{21} increased from 0.73 to 4.85%, A_{22} from 1.43 to 4.3%, and A_{23} declined from 97.84 to 90.85% as the temperature increased to 65 °C. The collagen proteins denature upon heating, and thus, results in the structure change must affect the water status and it distributed with the sea cucumber body wall. Water mobility decreased with the increasing heating temperature. These results indicated that the heating of body wall could lead to free water shifting to bound water, especially more than 55 °C, thus resulted in shrinkage of sea cucumber.

As a rapid, direct, accurate imaging technique for food processing analysis, MRI not only can determine the water distribution in food samples, but also can visualize internal structural changes during the processing (Liu et al. 2013). Figure 2a shows the T_1 and T_2 weighted images of sea cucumber body wall heated at 35, 45, 55, and 65 °C, respectively, by using a sample at room temperature (25 °C) as control. It is of special interest to observe that the pseudo-color images more intuitively show the differences in each sample (high proton density, red color; low proton density, blue color). T_1-weighted images emphasize the area where a low mobility proton is present while T_2-weighted images emphasize the area where a high mobility proton is present (Hong et al. 2009). From the T_1-weighted MRI images, it was clear that the maps of the sea cucumber body wall change from blue to red with the increase of heating temperature. This demonstrated that the water in sea cucumber body wall at higher temperature was mainly bound water (T_1-weighted images). Moreover, the maps of T_2-weighted images shifted from red to blue as the temperature increased, further indicating that the degrees of proton freedom decreased upon the temperature increase, that is, from free water to bound water transition. Noticeably, there was a significant change associated with the decrease of free water when the body wall was heated at approximately 45 °C as shown in the T_2-weighted images. The water distribution became relatively uniform after the body wall samples were heated at 55 °C. Quantitatively, the relative intensity of the T_1- and T_2-weighted images displayed in Fig. 2b. The overall trend was the intensity of the T_2-weighted images decreased while T_1-weighted images increased with increasing of heating temperature. Similarly, a significant change of the relative intensity was observed between the temperatures 45 and 55 °C. The result was consistent with the trend of previously mentioned A_{21} and A_{23}. It is possible to infer that heating will lead to the loss of excessive extracellular space, thus decreasing the water-holding capacity of sea cucumber body wall.

Fig. 2 T_1- and T_2-weighted images (**a**) and corresponding histogram of the relative intensity of the T_1- and T_2-weighted images (**b**) of sea cucumber body wall after heating at different temperature for 30 min. A, B, a, b denote significant ($p < 0.05$) differences
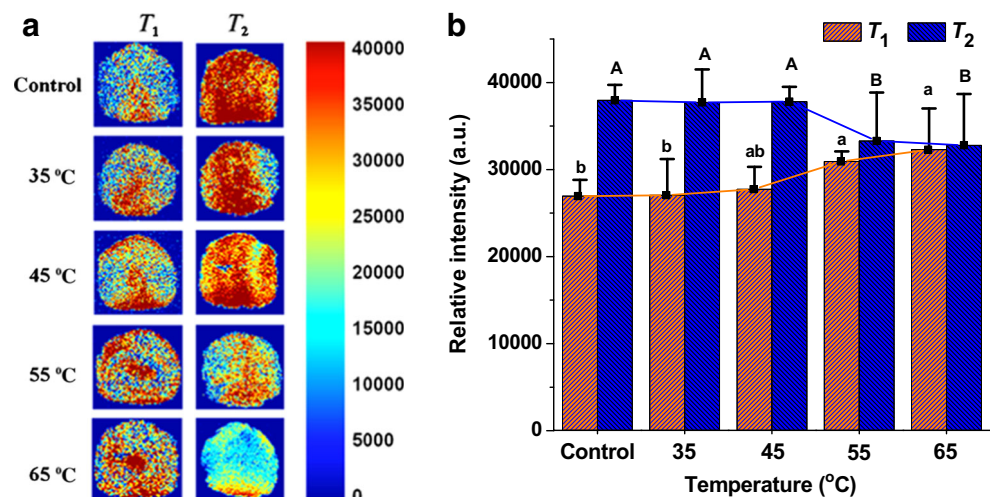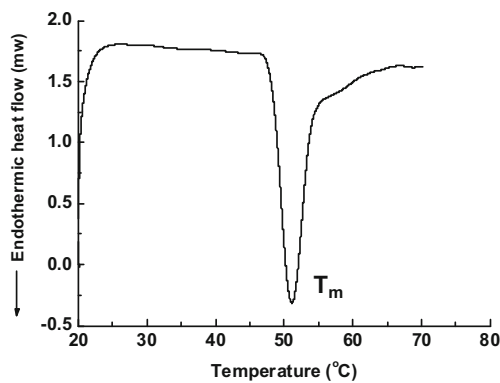
Fig. 3 Differential scanning calorimetry (DSC) thermogram of sea cucumber pastes

DSC Analysis and Dynamic Rheological Study

DSC analysis was also employed to character the structure change of the sea cucumber body wall. Figure 3 presents low-temperature heating profile of sea cucumber body wall heated from 20 to 70 °C. A prominent peak centered at around 51 °C (T_{max}) was observed with T_{onset} at about 45 °C. The net heat energy (enthalpy, $\triangle H$) was 1.442 (J/g). DSC detects endothermic peaks representing heat uptake by the protein structure as it gradually unfolds upon heating and transitions into its denatured structure. Studies on chicken and beef muscle showed that there are typically three peaks, in which the first peak corresponds to endothermic transition of myosin (~40–60 °C), the second to sarcoplasmic protein and collagen (~60–70 °C), and the third to actin (~80 °C) (Bertram et al. 2006). The body wall of sea cucumber *S. japonicas* is mainly composed of highly insolubilized collagen fibers (Saito et al. 2002). Herein, the DSC analysis showed only an endothermic peak at around 51 °C, about 6 °C lower than that (57 °C) of pepsin-solubilized collagen extracted from body wall of the sea cucumber *S. japonicas* (Cui et al. 2007). The denaturation temperature of body wall is in the range of 45–55 °C which is in accordance with the result observed in NMR and MRI

analysis, further confirming the heat-induced changes in collagen structures.

The elastic behavior is another critical quality attribute which translates into textural properties of sea cucumber body wall during the low-temperature heating process. Thus, rheology was also employed in this study for quality control. A typical storage modulus (G′) pattern for sea cucumber paste was recorded to characterize transition from viscous protein paste to a solid (Fig. 4a). With the temperature increasing, the G′ showed only marginal change until 45 °C, followed by a marked increase which leveled at approximately 65 °C. The increase in G′ has been attributed to the ordered protein aggregation to form a three-dimensional gel network with water entrapped in the gel matrix (Dileep et al. 2005). This might have been due to denaturation of collagen protein structures induced by the low-temperature heating. It is crucial step for tenderization. The rheological properties showed similar trend to the DSC thermogram (Fig. 4), confirming that heating increases protein unfolding, leading to greater denaturation and eventually to the development of a more elastic gel. The changes in loss modulus G″ for body wall pastes were similar to those in their G′, although the magnitude of G″ values was much smaller. Tan δ of sea cucumber body wall gradually decreased from 0.46 to 0.13 when heated from 45 to 65 °C. These suggested that elastic gel body with proteins network structure formed gradually. Subsequently, a strong network developed after 65 °C. The change of these parameters with the lapse of time at 45 °C was shown in Fig. 4b. It can be seen that Tan δ decreased gradually with increasing the time. G′ and G″ started to increase from 15 min, reaching the highest peak at approximately 30 min. This demonstrated that it took about 30 min for the body wall collagen to form a gel network at 45 °C.

Enzymatic Assay

During low-temperature heating process, the sea cucumber body wall went through structural denaturation and solubilization. Ringer's soluble fraction (RSF) is the fraction of
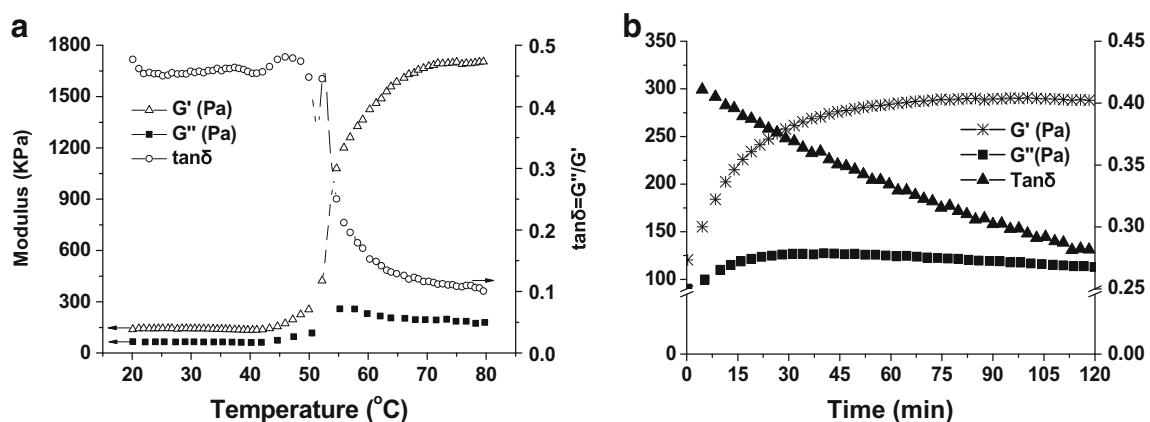

Fig. 4 Dynamic rheological properties of sea cucumber paste at different temperature (a) and different time (b)
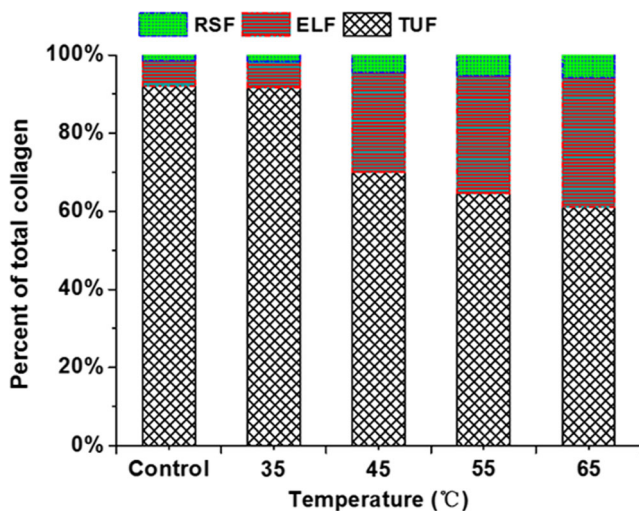
Fig. 5 Relative composition of collagen in sea cucumber body wall heated to 25 (control), 35, 45, 55, and 65 °C

collagen soluble in Ringer's solution as reported by the Hill procedure in 1966 (Hill 1966). The enzyme-labile fraction (ELF) is the part of the collagen molecule that is unprotected by the tight molecular configuration of native collagen. The total unaltered fraction (TUF) is the portion of collagen that has not been denatured enough for the quaternary structure of the molecule to be disturbed, thereby protecting it from enzyme attack (Powell et al. 2000). Therefore, the analysis of these fractions of sea cucumber body wall during low-temperature heating may provide more precise information on the cause of structure change and thus would further explain the changes observed in NMR and MRI. Figure 5 shows the changes in the collagen composition over heating treatments at different temperature. ELF increased from 6.54 to 33.10% as temperature increased from 25 to 65 °C (Table 2). ELF was indicative of the denaturation as the heating temperature increased (Powell et al. 2000). A significant increase of ELF was observed when the temperature reached 45 °C (Fig. 5), suggesting the separation of the heat-induced soluble portion from the insoluble. This is in

Table 2 Effect of heating on solubility enzyme lability on collagen in sea cucumber body wall

Temperature (°C)	Percent(±SD) of total collagen		
	RSF	ELF	TUF
Control (25 °C)	1.43[a] ± 0.18	6.54[a] ± 0.18	92.03[a] ± 8.11
35	1.53[a] ± 0.09	6.84[a] ± 0.35	91.63[a] ± 5.63
45	4.49[b] ± 0.48	25.51[b] ± 2.48	70.00[b] ± 6.49
55	5.34[c] ± 0.23	30.07[c] ± 0.55	64.58[bc] ± 5.78
65	5.77[d] ± 0.48	33.10[d] ± 1.20	61.13[d] ± 2.68

SD standard deviation

[a–d] Different letter superscripts in each column denote significant ($p < 0.05$) differences, respectively
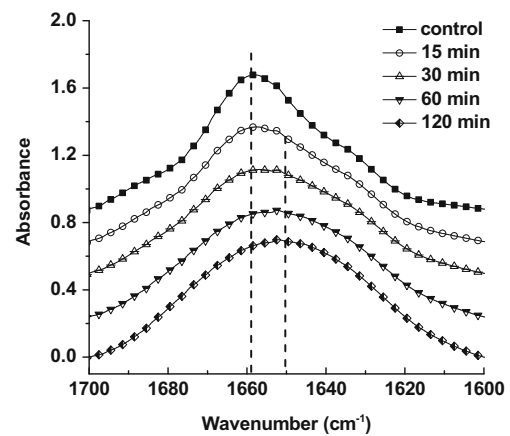

Fig. 6 Fourier transform infrared spectra of amid I (1700–1600 cm^{-1}) of collagen fibrils heated at 45 °C with various time of 15, 30, 60, 120 min

agreement with the fact observed in NMR and MRI analysis, inferring the occurrence of body wall structure change during the low-temperature heating treatment. TUF decreased ($p < 0.05$) as temperature increased from 35 to 65 °C also indicating that the partial quaternary structure of the collagen had been disturbed as tenderization occurred. Significant decrease of TUF was observed when the heating temperature was 45 °C as evident by NMR and MRI. Moreover, RSF remained relatively constant. The relatively low amount of body wall collagen solubilization that occurred was expected, because this process normally leads to loss of collagen. There was only less than 6% RSF when the body wall samples were heated at 65 °C.

FT-IR of Sea Cucumber Collagen Fibrils

To further investigate the protein structure change of the sea cucumber body wall, FT-IR spectroscopy was applied to characterize collagen fibrils heated at 45 °C for up to 120 min. Figure 6 shows the typical Fourier transform infrared spectra of amid I (1700–1600 cm^{-1}) of collagen fibrils heated at 45 °C with various time. Amide I region was selected in the characterization of protein secondary structure change during low-temperature heating at 45 °C. The amide I region is dominated by carbonyl stretching vibrations with minor contributions from C–N stretching and N–H bending (Sano et al. 1994). A component centered between approximately 1658 and 1650 cm^{-1} has been assigned to the α-helix (Kr 1986). More than one β-component has been observed in the spectra of many β-sheet proteins. Bands in the regions of 1640–1620 and 1695–1690 cm^{-1} have been assigned to β-sheet by many authors (Lee et al. 1990; Susi and Byler 1986). The assignment of bands around 1670, 1683, 1688, and 1694 cm^{-1} to β-turns has been proposed (Kr 1986). In the present study, the maximum intensity of the 1658 cm^{-1} band in the spectra of the collagen fibrils can be attributed to proteins with high α-helix content (Fig. 6). The intensity maximum of this band shifted
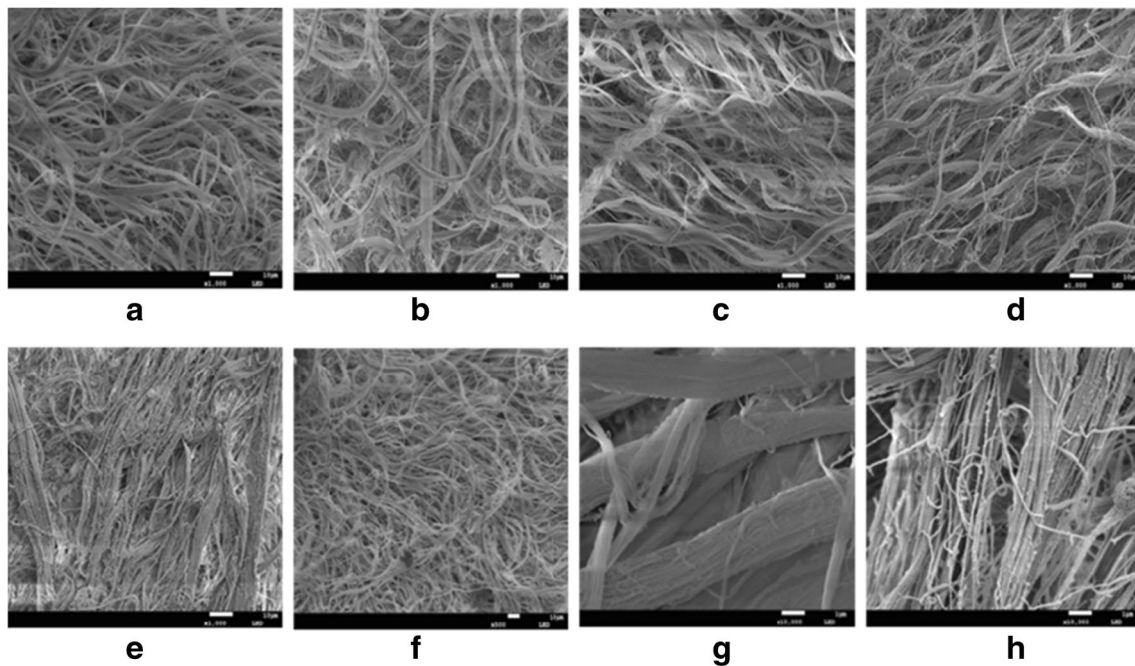
Fig. 7 Views of raw and heated sea cucumber by a scanning electron micrographic (SEM). **a** Raw sample, **b** heating for 15, **c** 30, **d** 60, **e** 120 min; **a–e** ×1000, **f** raw sample, ×500, **g** raw sample, ×10,000, **h** heating for 120 min, ×10,000. All treatments were carried out at 45 °C

hugely to lower frequencies after heating 15 min. This means that heating increased the β-sheet fraction for all heat-induced samples. Peak shape also changed obviously. A reasonable explanation for the band change may be a decrease in α-helix content and possible formation of other secondary structures resulting from heat treatment (Liu et al. 2008). In accordance with the NMR and MRI analysis, the FT-IR result revealed a gradual on-going structural change of collagen fibrils, the body wall main component, when heated at 45 °C for 30 min.

Microstructure Characterization

Microstructures of raw and heated sea cucumber body wall samples were examined using scanning electron microscope (SEM). As shown in Fig. 7, the fibers of raw sample were longer, and their distribution was in a certain direction (Fig. 7a, f, g). In contrast, body wall fibers after heating for 15 min bent and shrank, and the space between the fibers increased (Fig.7b). With increasing heating time, this trend continued up to 60 min (Fig. 7c, d). The collagen fibrils wrapped or twisted with each other and complete fiber bundle in tissue ruptured and then formed close structure. After heating for 120 min, (Fig. 7e, h), the fibers in long-time heated samples changed from coarseness to fineness. Most of the fibers became very relaxed, stretched, thinner, and nearly parallel ordered with each other. A similar result was also reported previously (Liu et al. 2012), which found that fiber bundles in raw sample were rich and loosely, and aggregated and the gaps between fibers became smaller after heating at 50 °C. This result indicated that the low-temperature heating did

induce microstructure changes, which might be closely related to the proton density and distribution change. Relaxation times were concerned with fine porous microstructure where the water molecules was restricted in their motion due to smaller pores in the network structure (Han et al. 2009; Salomonsen et al. 2007). Thus, the NMR and MRI may provide a fast and non-invasive assessment of the microstructure changes during heating process for better food quality control.

Relationship Analysis

In order to investigate the relationship between the heating temperature, gel properties (dynamic rheological properties), and NMR analysis, Pearson correlation analysis test was used

Table 3 Correlation between NMR parameters and temperature, G′, RSF, ELF, and TUF

	Temperature	G′	RSF	ELF	TUF
Temperature	1.00[c]	0.899[a]	0.945[a]	−0.942[a]	−0.942[a]
T_{21}	−0.983[b]	0.815	−0.914[a]	−0.911[a]	0.911[a]
T_{22}	−0.712	−0.738	−0.467	−0.463	0.464
T_{23}	−0.782	−0.854	−0.609	−0.609	0.608
A_{21}	0.919[a]	0.980[b]	0.815	0.811	−0.812
A_{22}	0.848	0.832	0.834	0.823	−0.825
A_{23}	−0.947[a]	−0.972[b]	−0.883[a]	−0.875	0.876
T_1 intensity	0.937[a]	0.994[c]	0.870	0.865	−0.865
T_2 intensity	−0.886[a]	−0.988[c]	−0.81	−0.801	0.802

[a] $p < 0.05$, [b] $p < 0.01$, [c] $p < 0.001$

to analyze the relationship between the NMR relaxation parameters and physicochemical properties. As a fast and non-invasive analytical technique, NMR can in many cases replace the more time-consuming and sample destructive analysis methods if strong correlations between the NMR parameters and relative physicochemical parameters are found. As shown in Table 3, T_{21} was highly positively correlated with TUF and negatively correlated with temperature, RSF, and ELF ($p < 0.01$ or $p < 0.05$). T_{22} and T_{23} were not highly correlated with any physicochemical parameters. A_{21} was highly positively correlated with temperature and G′, while A_{23} was highly negatively correlated with temperature, G′ and RSF. T_1 intensity was highly positively, while T_2 intensity was negatively correlated with temperature and G′. The results indicated that heat-induced protein in body wall would cause significant changes in body wall physicochemical properties. The high correlation coefficient between the physicochemical properties and NMR parameters of body wall indicated that low-field NMR and MRI might have potential for fast and non-invasive assessment of sea cucumber body wall changes. Thereby, the correlation values suggested that it might be possible to substitute instrumental methods that determine G′, RSF, ELF, and TUF by low-field NMR for monitoring the heat-induced changes in collagen structures of sea cucumber body wall in a rapid and non-invasive manner.

Conclusions

Low-field NMR and MRI could be used as a fast and non-invasive method for the assessment of the tenderization of sea cucumber body wall. NMR relaxometry enables probing the mobility of protons, and MRI could visualize internal structural changes during the low-temperature heating process, thereby providing useful information about interactions between myowater and the collagen proteins. Measurements made through LF-NMR and MRI demonstrated a significant change of the sea cucumber body wall when heated between 45 and 55 °C. The changes observed by NMR technique were also confirmed by DSC, FTIR, and SEM measurements. Strong correlations between the NMR parameters and rheology storage modulus (G′), relative enzymatic assay parameters, RSF, ELF, and TUF, were found for the low-temperature tenderization of sea cucumber body wall. All these results herein revealed that it could be possible to use NMR and MRI to assess sea cucumber tenderization during low-temperature heating process.

Conflicts of Interest Xiuping Dong declares that he has no conflict of interest. Yan Li declares that he has no conflict of interest. Yong Li declares that he has no conflict of interest. Liang Song declares that he has no conflict of interest. Shasha Cheng declares that he has no conflict of interest. Dongmei Li declares that he has no conflict of interest. Weibei Zhu declares that he has no conflict of interest. Dayong Zhou declares that he has no conflict of interest. Mingqian Tan declares that he has no conflict of interest.

Ethical Approval This article does not contain any studies with human participants or laboratory animals performed by any of the authors.

Informed Consent Not applicable.

References

Bertram HC, Wu Z, Berg FVD, Andersen HJ (2006) NMR relaxometry and differential scanning calorimetry during meat cooking. Meat Sci 74:684–689. doi:10.1016/j.meatsci.2006.05.020

Carneiro CDS, Mársico ET, Ribeiro RDOR, Conte Júnior CA, Álvares TS, De Jesus EFO (2013) Quality attributes in shrimp treated with polyphosphate after thawing and cooking: a study using physicochemical analytical methods and low-field1H NMR. J Food Process Eng 36:492–499. doi:10.1111/jfpe.12011

Cui F-X, Xue C-H, Li Z-J, Zhang Y-Q, Dong P, Fu X-Y, Gao X (2007) Characterization and subunit composition of collagen from the body wall of sea cucumber *Stichopus japonicus*. Food Chem 100:1120–1125. doi:10.1016/j.foodchem.2005.11.019

Dileep A, Shamasundar B, Binsi P, Badii F, Howell N (2005) Effect of ice storage on the physicochemical and dynamic viscoelastic properties of ribbonfish (Trichiurus spp) meat. J Food Sci 70:E537–E545. doi:10.1111/j.1365-2621.2005.tb08316.x

Geng S, Wang H, Wang X, Ma X, Xiao S, Wang J, Tan M (2015) A non-invasive NMR and MRI method to analyze the rehydration of dried sea cucumber. Anal Methods-UK 7:2413–2419. doi:10.1039/C4AY03007A

Goetz J, Koehler P (2005) Study of the thermal denaturation of selected proteins of whey and egg by low resolution NMR. LWT-Food Sci Technol 38:501–512. doi:10.1016/j.lwt.2004.07.009

Han M, Zhang Y, Fei Y, Xu X, Zhou G (2009) Effect of microbial transglutaminase on NMR relaxometry and microstructure of pork myofibrillar protein gel. Eur Food Res Technol 228:665–670. doi:10.1007/s00217-008-0976-x

Herrero AM, Carmona P, García ML, Solas MT, Careche M (2005) Ultrastructural changes and structure and mobility of myowater in frozen-stored hake (*Merluccius merluccius* L.) muscle: relationship with functionality and texture. J Agric Food Chem 53:2558–2566. doi:10.1021/jf0490706

Hill F (1966) The solubility of intramuscular collagen in meat animals of various ages. J Food Sci 31:161–166. doi:10.1111/j.1365-2621.1966.tb00472.x

Hong Y-S, Cho J-H, Kim N-R, Lee C, Cheong C, Hong KS, Lee C-H (2009) Artifacts in the measurement of water distribution in

soybeans using MR imaging. Food Chem 112:267–272. doi:10.1016/j.foodchem.2008.05.109

Kim S-K, Himaya S (2012) Triterpene glycosides from sea cucumbers and their biological activities. Adv Food Nutr Res 65:297–319. doi:10.1016/B978-0-12-416003-3.00020-2

Kr S (1986) Vibrational spectroscopy and conformation of peptides, polypeptides, and proteins. Adv Protein Chem 38:181–364

Lee DC, Haris PI, Chapman D, Mitchell RC (1990) Determination of protein secondary structure using factor analysis of infrared spectra. Biochemist 29:9185–9193. doi:10.1021/bi00491a012

Leikina E, Mertts M, Kuznetsova N, Leikin S (2002) Type I collagen is thermally unstable at body temperature. P Natl Acad Sci USA 99: 1314–1318. doi:10.1073/pnas.032307099

Li C, Liu D, Zhou G, Xu X, Qi J, Shi P, Xia T (2012) Meat quality and cooking attributes of thawed pork with different low field NMR T 21. Meat Sci 92:79–83. doi:10.1016/j.meatsci.2011.11.015

Liu J, Zhu K, Ye T, Wan S, Wang Y, Wang D, Li B, Wang C (2013) Influence of konjac glucomannan on gelling properties and water state in egg white protein gel. Food Res Inter 51:437–443. doi:10.1016/j.foodres.2013.01.002

Liu L, Zhang Z, Liu Q, Yang B, Huang J, Gao X (2012) Rheological and structural properties of sea cucumber *Stichopus japonicus* during different heating temperature. Int J Fish Aquaculture 4:209–216. doi:10.5897/IJFA12.027

Liu R, Zhao S-M, Xiong S-B, Xie B-J, Qin L-H (2008) Role of secondary structures in the gelation of porcine myosin at different pH values. Meat Sci 80:632–639. doi:10.1016/j.meatsci.2008.02.014

Lomiwes D, Farouk M, Wu G, Young O (2014) The development of meat tenderness is likely to be compartmentalised by ultimate pH. Meat Sci 96:646–651. doi:10.1016/j.meatsci.2013.08.022

Marcone MF, Wang S, Albabish W, Nie S, Somnarain D, Hill A (2013) Diverse food-based applications of nuclear magnetic resonance (NMR) technology. Food Res Inter 51:729–747. doi:10.1016/j.foodres.2012.12.046

Nagai T, Suzuki N (2000) Isolation of collagen from fish waste material - skin, bone and fins. Food Chem 68:277–281. doi:10.1016/S0308-8146(99)00188-0

Naganathan GK, Grimes LM, Subbiah J, Calkins CR, Samal A, Meyer GE (2008) Visible/near-infrared hyperspectral imaging for beef tenderness prediction. Comput Electron Agr 64:225–233. doi:10.1016/j.compag.2008.05.020

Nakano S, Kousaka J, Fujii K, Yorozuya K, Yoshida M, Mouri Y, Akizuki M, Tetsuka R, Ando T, Fukutomi T, Oshima Y, Kimura J, Ishiguchi T, Arai O (2012) Impact of real-time virtual sonography, a coordinated sonography and MRI system that uses an image fusion technique, on the sonographic evaluation of MRI-detected lesions of the breast in second-look sonography. Breast Cancer Res Treat 134: 1179–1188. doi:10.1007/s10549-012-2163-9

Patel KK, Khan MA, Kar A (2015) Recent developments in applications of MRI techniques for foods and agricultural produce—an overview. J Food Sci Technol MYS 52:1–26. doi:10.1007/s13197-012-0917-3

Powell T, Hunt M, Dikeman M (2000) Enzymatic assay to determine collagen thermal denaturation and solubilization. Meat Sci 54: 307–311. doi:10.1016/S0309-1740(99)00092-3

Rabotyagova OS, Cebe P, Kaplan DL (2008) Collagen structural hierarchy and susceptibility to degradation by ultraviolet radiation. Mat Sci Eng C-Mater 28:1420–1429. doi:10.1016/j.msec.2008.03.012

Sánchez-Valencia J, Sánchez-Alonso I, Martinez I, Careche M (2015) Low-field nuclear magnetic resonance of proton (1H LF NMR) relaxometry for monitoring the time and temperature history of frozen hake (*Merluccius merluccius* L.) muscle. Food Bioprocess Tech 8:2137–2145. doi:10.1007/s11947-015-1569-x

Saito M, Kunisaki N, Urano N, Kimura S (2002) Collagen as the major edible component of sea cucumber (*Stichopus japonicus*). J Food Sci 67:1319–1322. doi:10.1111/j.1365-2621.2002.tb10281.x

Salomonsen T, Sejersen MT, Viereck N, Ipsen R, Engelsen SB (2007) Water mobility in acidified milk drinks studied by low-field 1 H NMR. Intl Dairy J 17:294–301. doi:10.1016/j.idairyj.2006.04.003

Sano T, Ohno T, Otsuka-Fuchino H, Matsumoto JJ, Tsuchiya T (1994) Carp natural actomyosin: thermal denaturation mechanism. J Food Sci 59:1002–1008. doi:10.1111/j.1365-2621.1994.tb08177.x

Santos PM, Corrêa CC, Forato LA, Tullio RR, Cruz GM, Colnago LA (2014) A fast and non-destructive method to discriminate beef samples using TD-NMR. Food Control 38:204–208. doi:10.1016/j.foodcont.2013.10.026

Shaarani SM, Nott KP, Hall LD (2006) Combination of NMR and MRI quantitation of moisture and structure changes for convection cooking of fresh chicken meat. Meat Sci 72:398–403. doi:10.1016/j.meatsci.2005.07.017

Shao X, Li Y (2010) Classification and prediction by LF NMR. Food Bioprocess Tech 5:1817–1823. doi:10.1007/s11947-010-0455-9

Susi H, Byler DM (1986) Resolution-enhanced Fourier transform infrared spectroscopy of enzymes. Method Enzymol 130:290–311. doi:10.1016/0076-6879(86)30015-6

Van Laack R, Stevens S, Stalder K (2001) The influence of ultimate pH and intramuscular fat content on pork tenderness and tenderization. J Anim Sci 79:392–397. doi:10.2527/2001.792392x

Yearbook CFS (2009) China fishery statistical yearbook 2008. Fisheries Bureau, Department of Agriculture of China, Beijing (in Chinese)

Yogesh K, Ali J (2014) Effect of mung bean and sprouted mung bean (*Vigna radiata*) powder on chicken breast meat tenderness, microbial and sensory characteristics. J Food Sci Tech 51:1411–1415. doi:10.1007/s13197-012-0650-y

Zhang L, McCarthy MJ (2012) Black heart characterization and detection in pomegranate using NMR relaxometry and MR imaging. Postharvest Biol Tec 67:96–101. doi:10.1016/j.postharvbio.2011.12.018

Zhang L, McCarthy MJ (2013) NMR study of hydration of navy bean during cooking. LWT-Food Sci Technol 53:402–408. doi:10.1016/j.lwt.2013.03.011

Zhou D-Y, Chang X-N, Bao S-S, Song L, Zhu B-W, Dong X-P, Zong Y, Li D-M, Zhang M-M, Liu Y-X (2014) Purification and partial characterisation of a cathepsin L-like proteinase from sea cucumber (*Stichopus japonicus*) and its tissue distribution in body wall. Food Chem 158:192–199. doi:10.1016/j.foodchem.2014.02.105

Zhou Y, Yang H, Liu S, Yuan X, Mao Y, Liu Y, Xu X, Zhang F (2006) Feeding and growth on bivalve biodeposits by the deposit feeder *Stichopus japonicus* Selenka (Echinodermata: Holothuroidea) co-cultured in lantern nets. Aquaculture 256:510–520. doi:10.1016/j.aquaculture.2006.02.005

Zhu J, Wang D, Dong X, Zhu B (2013) Study on tenderization of sea cucumber (StichoPusjaPonicus) by low-temperature heating. In: Abstract of Food Summit in China 2013 & Annual meeting of Chinese Institte of Food Science and Technology (p. 64). Hangzhou China: Chinese Institte of Food Science and Technology